Petroleum Science 21 (2024) 315–326

Contents lists available at ScienceDirect

Petroleum Science

journal homepage: www.keaipublishing.com/en/journals/petroleum-science

Original Paper

The effects of various factors on spontaneous imbibition in tight oil reservoirs

Cheng Liu [a], Tian-Ru Wang [a], Qing You [a,*], Yue-Chun Du [a], Guang Zhao [b], Cai-Li Dai [b]

[a] School of Energy Resources, China University of Geosciences, Beijing, 100083, PR China
[b] School of Petroleum Engineering, China University of Petroleum, Qingdao, 266580, Shandong, PR China

ARTICLE INFO

Article history:
Received 29 May 2023
Received in revised form
22 September 2023
Accepted 26 September 2023
Available online 4 October 2023

Edited by Yan-Hua Sun

Keywords:
Tight oil reservoir
Spontaneous imbibition
Nuclear magnetic resonance
Slickwater fracturing fluid
Fluid utilization degree

ABSTRACT

Slickwater fracturing fluids have gained widespread application in the development of tight oil reservoirs. After the fracturing process, the active components present in slickwater can directly induce spontaneous imbibition within the reservoir. Several variables influence the eventual recovery rate within this procedure, including slickwater composition, formation temperature, degree of reservoir fracture development, and the reservoir characteristics. Nonetheless, the underlying mechanisms governing these influences remain relatively understudied. In this investigation, using the Chang-7 block of the Changqing Oilfield as the study site, we employ EM-30 slickwater fracturing fluid to explore the effects of the drag-reducing agent concentration, imbibition temperature, core permeability, and core fracture development on spontaneous imbibition. An elevated drag-reducing agent concentration is observed to diminish the degree of medium and small pore utilization. Furthermore, higher temperatures and an augmented permeability enhance the fluid flow properties, thereby contributing to an increased utilization rate across all pore sizes. Reduced fracture development results in a lower fluid utilization across diverse pore types. This study deepens our understanding of the pivotal factors affecting spontaneous imbibition in tight reservoirs following fracturing. The findings act as theoretical, technical, and scientific foundations for optimizing fracturing strategies in tight oil reservoir transformations.

1. Introduction

The rapid advancement of the society and economy cannot be achieved without a stable supply of energy. Consequently, the demand of oil consumption is increasing at a rapid rate (Lei et al., 2019; Liu et al., 2024; Zheng et al., 2022; Zou et al., 2013). With the development of conventional oil reservoirs entering the end stage, unconventional energy represented by tight oil reservoirs has been vigorously developed and has gradually become a focus area of global attention (Zou, 2013; Zou et al., 2012). However, the poor reservoir properties and higher water injection pressure of tight reservoirs complicate their development by conventional means (Wu et al., 2022). Hydraulic fracturing is an effective approach to exploit tight reservoirs by creating artificial fractures in the formation to connect natural fractures and improve fluid flow channels, thus enhancing the flow capacity for the effective recovery of crude oil (Al-Muntasheri et al., 2018; Barati and Liang, 2014; Fall et al., 2015; Guo et al., 2015; Liu et al., 2020).

Slickwater fracturing fluid is a widely used low formation damage fracturing fluid (Abaa et al., 2022; Vishkai and Gates, 2019; Zhou et al., 2022). After fracturing with slickwater, there is no need to flowback, furthermore the slickwater can play a role in the imbibition and oil displacement within the formation. Thus, the slickwater energy is effectively utilized (Al-Muntasheri, 2014; King, 2012; Liu et al., 2022; Montgomery and Smith, 2010). Numerous factors can influence imbibition process in the tight reservoirs (Xia et al., 2021; Xu et al., 2019; Yang et al., 2019, 2023), including the concentration of the drag reducing agent in the slickwater fracturing fluid, the formation temperature, the reservoir rock permeability, and the fracture development degree in the reservoir (Guo et al., 2020; Hossain and Rahman, 2008; Li et al., 2023; Wang et al., 2020).

In tight oil reservoirs, the confined flow pathways present a challenge, where the introduction of molecules like polymers can significantly impact fluid mobility. Additionally, the intricate behavior of polymer solutions within tight cores warrants careful

* Corresponding author.
E-mail address: youqing@cugb.edu.cn (Q. You).

https://doi.org/10.1016/j.petsci.2023.09.022

Table 1
Ion concentration and salinity of the simulation formation water.

Ion concentration, mg/L				Total salinity, mg/L
Na^+	Ca^{2+}	Mg^{2+}	Cl^-	
3529.4	807.0	128.5	7260.3	11725.2

Table 2
Key parameters of core samples used.

Sample No.	Length, mm	Diameter, mm	Porosity, %	Permeability, mD
I-1	30.16	25.07	14.36	0.298
I-2	32.25	25.04	14.48	0.303
I-3	30.36	25.09	14.53	0.306
D-1	32.74	25.10	15.23	0.296
D-2	31.64	25.13	15.19	0.298
D-3	31.56	25.18	15.21	0.302
D-4	32.36	25.03	15.16	0.304
T-1	31.63	25.15	14.99	0.307
T-2	32.35	25.12	15.13	0.299
T-3	31.63	25.05	14.94	0.304
P-1	32.54	25.08	15.23	0.034
P-2	31.63	25.03	14.91	0.097
P-3	32.75	25.16	15.09	0.388
P-4	32.64	25.06	14.97	0.532
P-5	31.36	25.11	15.16	1.226
F-1	19.12	25.13	14.86	0.302
F-2	30.44	25.12	14.88	0.302
F-3	48.37	25.12	14.91	0.304

consideration. Noteworthy insights arise from the past research, which effectively showcases the viability of polymer flooding within tight rock cores with permeabilities below 5 mD, highlighting the proficient migration of polymer molecules within such formations. This migration, however, exerts discernible influence on the imbibition process (Haynes et al., 2013; Leon et al., 2018; Rachapudi et al., 2020). Notably, Song et al. emphasized that during the polymer migration in tight rock cores with residual oil, polymer retention surpassed the result of the core saturated with pure water, this result attributed to the constriction of smaller pore spaces during polymer migration (Song et al., 2021). In our preceding investigations, we explored a nanoparticle-enhanced slickwater (Liu et al., 2022). Our imbibition experiments conducted in tight rock core samples (~1 mD) yielded intriguing results. The experimental results indicate that the recovery rate of the imbibition fluid with pure nanoparticles is 1.8% higher than that of nanoparticle-enhanced slickwater. This marginal reduction in imbibition recovery is attributed to the possible obstruction of rock pore networks by specific components, which function as friction-reducing agents, in the slickwater fracturing fluid.

Research on the effects of different factors in the imbibition procedure using conventional means is limited by the poor physical properties and low porosity of matrix in tight reservoirs (Cai et al., 2020; Cheng et al., 2019; Dai et al., 2019). Hydrogen atoms have a high magnetic spin rate and are abundant in organic molecules and water. Moreover, the distribution of organic molecules or water can be effectively characterized by the detection of hydrogen atoms. In particular, the distribution of organic and water molecules in a sample can be determined by applying a magnetic field to the sample, allowing for the detection of the interaction between the hydrogen atoms and the magnetic field. This is the basic principle of nuclear magnetic resonance (NMR), a spatially nondestructive method that does not damage the sample (Liu et al., 2023).

In the development of tight reservoirs, many conventional investigation tools cannot be used due to the poor physical properties of the reservoirs. Thus, NMR scanning analysis is increasingly used to evaluate reservoir properties as it can effectively determine the distribution of fluids within the pore space by shielding the hydrogen signal in the oil or water phase (Jiang et al., 2022, 2023; Tang et al., 2023). In experimental settings, the introduction of heavy water (D_2O) is a well-established approach to selectively screen water molecules. This facilitates the identification of occurrences and shifts within the oil phase. Similarly, the incorporation of fluorine oil serves to shield the oil phase, thereby enabling the monitoring of injection and displacement dynamics within the water phase (Wu et al., 2020).

In this study, the Chang-7 block of the Changqing Oilfield is selected as the target reservoir, with the EM-30 slickwater fracturing fluid as the study object. The reservoir and crude oil

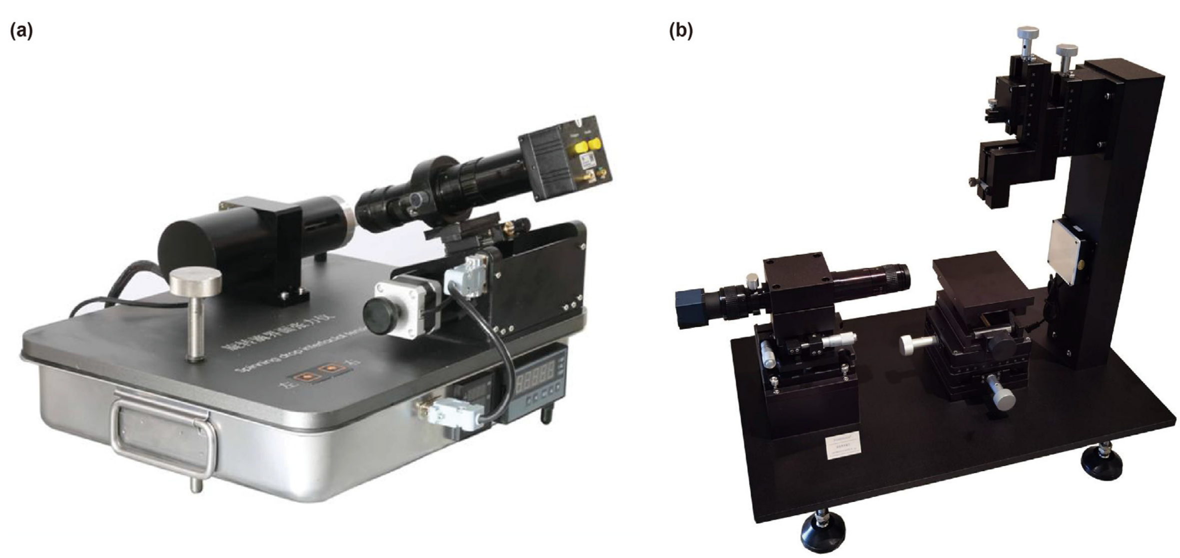

Fig. 1. Interfacial tension meter and contact angle meter.

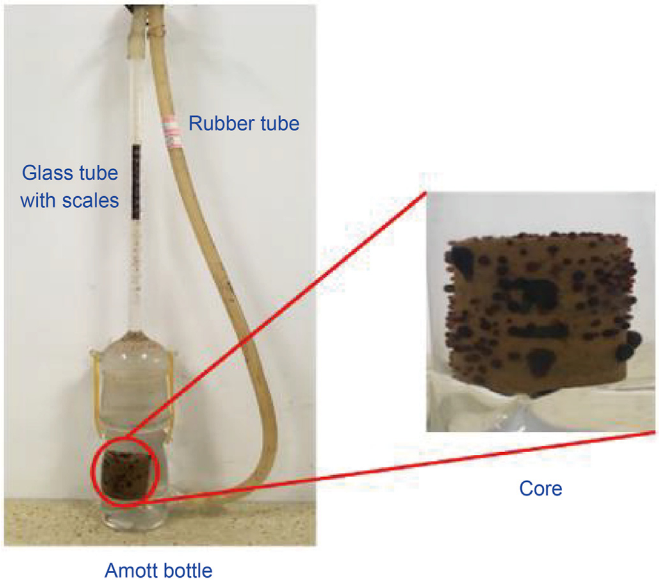

Fig. 2. The Amott bottle used in the experiment.

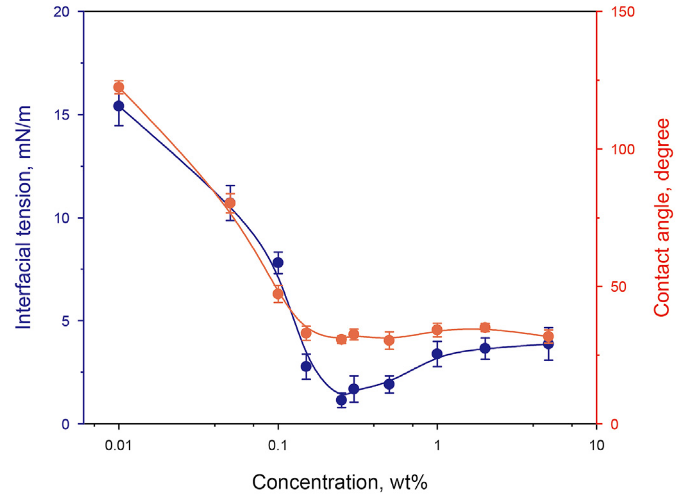

Fig. 4. Interfacial performance of the slickwater: Interfacial tension and contact angle.

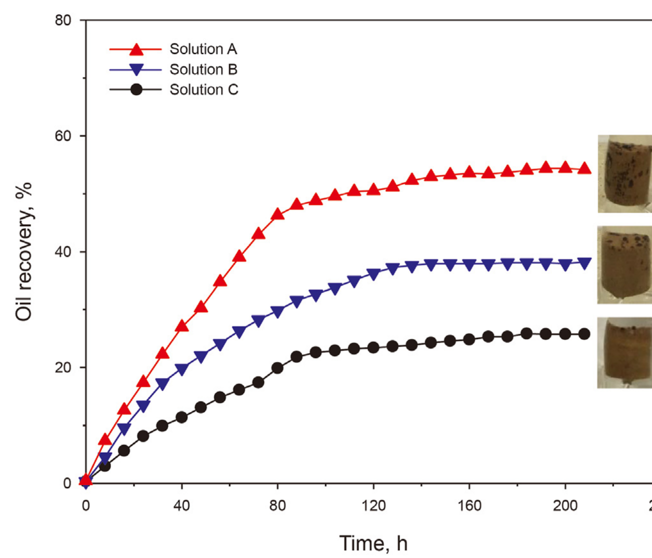

Fig. 5. Oil recovery of the imbibition experiments.

properties are combined, and static imbibition experiments and an online NMR system are used to evaluate the basic performance of the slickwater fracturing fluid. The effects of drag reducing agent concentration, temperature, core permeability, and core fracture development on the static imbibition process of slickwater are then investigated to clarify the utilization degree and utilization pattern of macro, medium and small pores in the core under the influence of different factors. The purpose of this paper is to provide theoretical support and a scientific basis for fracture modification using slickwater fracturing fluid in tight reservoirs.

2. Materials and methods

2.1. Materials

EM30 is a drag reducing agent in slickwater with a polyacrylamide-type polymer of a comb-like molecular structure. T-2 has an interfacial tension and contact angle equilibrium value suitable for a drainage aid agent, while T-1 is an effective anti-swell agent with multiple cationic sites and is abundant in hydroxyl groups. Table 1 reports the simulated formation water composition used in the experiment. NaCl (AR, 99.5%), $CaCl_2$ (AR, 96.0%), and $MgCl_2 \cdot 6H_2O$ (AR, 98.0%) were purchased from Sino-pharm Chemical Reagent Co., Ltd (Shanghai, China).

Degasified and dehydrated crude oil from the Chang-7 block of the Ordos Basin at the Changqing Oilfield was employed for the experiment, with a density of 0.8436 g/cm^3 and a viscosity of

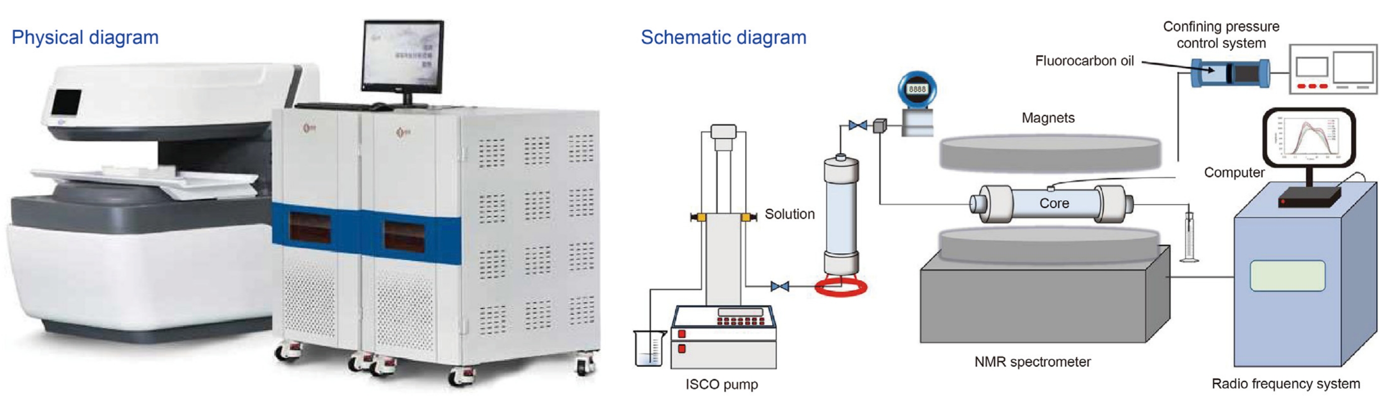

Fig. 3. The schematic and physical diagrams of the NMR experimental set-ups.

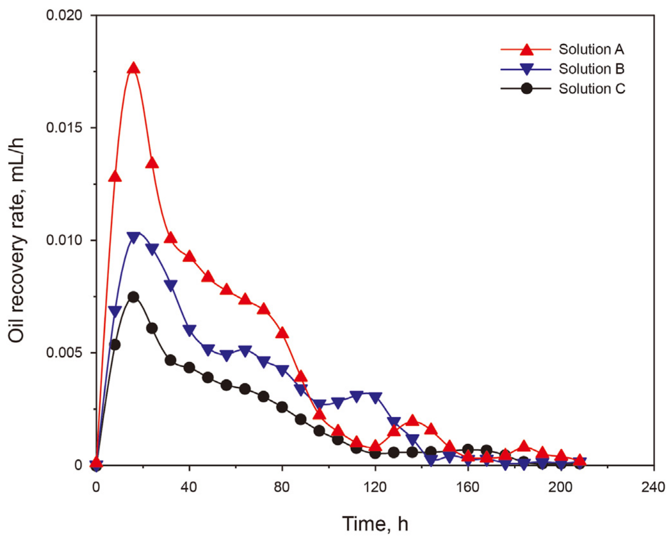

Fig. 6. Imbibition recovery rate under varying imbibition fluid conditions.

4.1 mPa s at 60 °C. The cores used in the experiment are also from the Chang-7 block and their key parameters are listed in Table 2.

2.2. Methods

2.2.1. Interfacial performance measurements

Among the components of slick water fracturing fluids, surfactant-type drainage aids are used to reduce the interfacial tension and improve the rock surface wettability. The oil–water interfacial tension between the oil and drainage aid with different concentrations was measured by a rotating drop interfacial tensiometer (TX-500C, CNG company, USA, Fig. 1(a)) with 6000 r/min at 60 °C. The contact angle between the drainage aid solutions/oil-droplet/core piece were measured using a contact angle measuring instrument (JC-2000D, Shanghai Zhongchen Digital Technic Apparatus Co., Ltd, China, Fig. 1(b)) at 60 °C. The solvents used in the experiments were simulated formation water.

2.2.2. Static imbibition experiment

The imbibition experiment was performed in an Amott bottle (Fig. 2). The upper part of the bottle contained a glass tube with scale and the lower part was filled with the core sample and imbibition solution. A rubber tube was used to inject the solution into the lower part of the bottle. The experimental procedure is summarized as follows:

(1) A 3-cm-long-core was cut by a core cutter, cleaned, dried, and weighted.

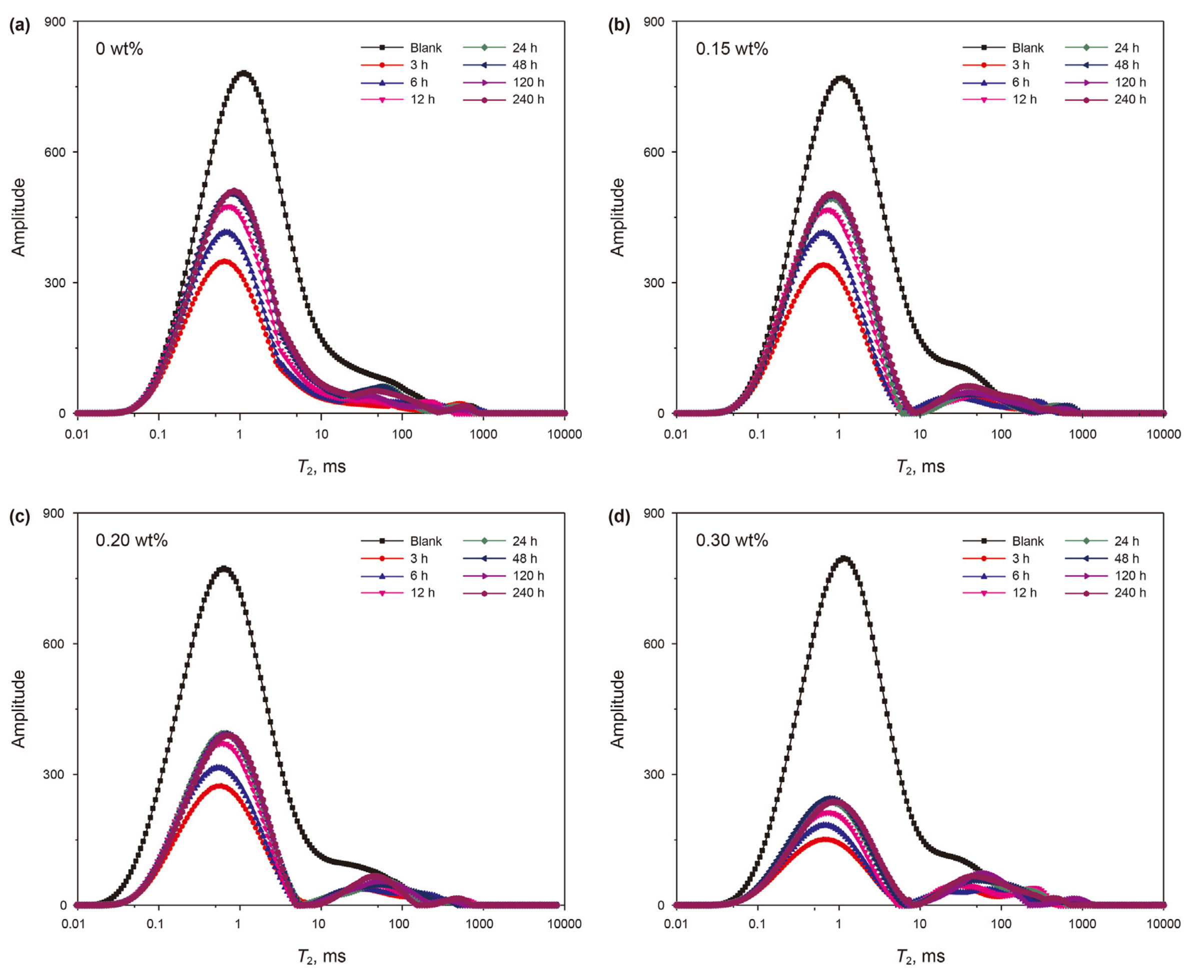

Fig. 7. Impact of the drag reducing agent concentration on spontaneous imbibition.

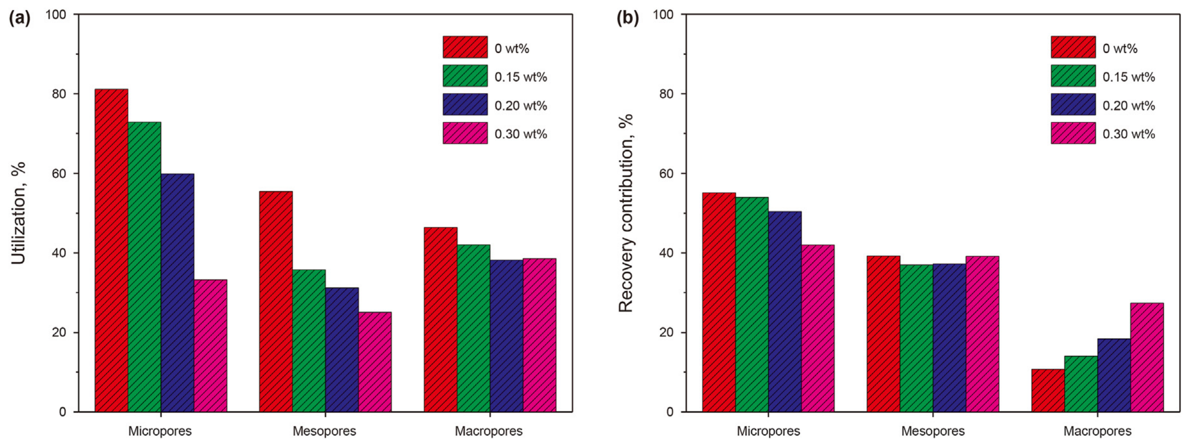

Fig. 8. Fluid utilization and recovery contribution of different pore sizes.

(2) The core was pumped to a vacuum by a vacuum pumping machine and subsequently pressurized and saturated with crude oil. The core was then stored at a temperature of 60 °C.
(3) The core was removed, the oil on the surface was cleaned and the weight of the core was recorded.
(4) The core was placed into the Amott bottle and the bottle was sealed with petroleum jelly. The imbibition solution was injected into the Amott bottle through the rubber tube. The device was placed in a constant temperature water bath at 60 °C.
(5) The crude oil volume in the glass tube was read periodically and the imbibition recovery was calculated using Eq. (1).

$$R_{\mathrm{I}} = \frac{\rho V}{m_2 - m_1} \times 100\% \tag{1}$$

where R_{I} is the imbibition recovery of the core, %; ρ is the oil density, g/cm^3; V is the volume of the oil observed on the glass tube, mL; m_2 is the mass of the core measured in step (3), g; and m_1 is the mass of the core measured in step (1), g.

2.2.3. Online NMR imbibition experiment

Using the online NMR equipment to study the degree of crude oil utilization in cores under different conditions, the impacts of different factors on the static imbibition process of slickwater fracturing fluid were investigated at the microscopic pore scale. Fig. 3 presents the schematic and physical diagrams of the experimental set-ups. The system was composed of an MacroMR low-field NMR detector (Suzhou Niumag Analytical Instrument Co., Ltd, China), a nuclear magnetic analysis system (Suzhou Niumag Analytical Instrument Co., Ltd, China), and a core displacement system.

Nuclear magnetic resonance scanning is a spatial nondestructive testing tool that has been increasingly applied to the study of low-permeability tight cores in recent years. Research is typically performed using the time required for the transverse decay component of the non-equilibrium magnetization vector of a hydrogen nucleus to reach zero under the action of an applied magnetic field. More specifically, the transverse relaxation time T_2 is taken as the detection signal. Here T_2 is calculated as follows:

$$\frac{1}{T_2} = \frac{1}{T_{2\mathrm{S}}} + \frac{1}{T_{2\mathrm{B}}} + \frac{1}{T_{2\mathrm{D}}} \tag{2}$$

where T_2 is the transverse relaxation time; $T_{2\mathrm{S}}$ is the surface relaxation time, which is determined by the matrix pore size and decreases with the pore size; $T_{2\mathrm{B}}$ is the body relaxation time determined by the fluid properties and is typically a constant value used to identify the fluid; and $T_{2\mathrm{D}}$ is the diffusion relaxation time. Note that under low magnetic field single fluid conditions, the effect of $T_{2\mathrm{D}}$ on the transverse relaxation time is essentially negligible. Thus, the variation in T_2 is typically affected by $T_{2\mathrm{S}}$, namely, the pore size. There is also a positive correlation between the variation in $T_{2\mathrm{S}}$ and pore size. According to Eq. (2), T_2 rises with the pore size and corresponds to different pore throat sizes. Furthermore, the NMR experiments are generally based on the hydrogen signal intensity, with a higher intensity indicating a greater saturated fluid volume. The NMR scanning experiments can reveal the variation curve of the core hydrogen signal intensity with T_2. The hydrogen signal intensity at a certain relaxation time can characterize the saturated fluid volume at its corresponding pore size. This allows for the saturation of the saturated fluid within a certain pore size range to be determined using the integration operation. The key steps of the experimental procedure are as follows:

(1) The cores were processed and subsequently measured for weight, length, diameter, permeability, and porosity.
(2) The cores were initially evacuated to a vacuum state using a vacuum pump, then saturated with ultrapure water, and weighed. The cores saturated with ultrapure water were obtained.
(3) The saturated cores were placed in the measuring apparatus and the cores were analyzed for T_2 spectra using the NMR analysis system to obtain T_2 signals of the cores under blank conditions.
(4) After undergoing step (3) processing, the cores were dried again, and step (1) was repeated.
(5) The cores were initially evacuated to a vacuum state using a vacuum pump, then saturated with fluorine oil, and T_2 signals of the cores were tested using NMR to obtain the basal.
(6) After undergoing step (5) process, the cores were placed in slickwater for imbibition experiments.
(7) The cores at different experimental stages were removed and T_2 spectra of the core sample were measured using the NMR.

The NMR scanning parameters used to measure T_2 spectra were as follows: waiting time T_{w} of 2000 ms; number of scans N_{S} of 64; echo interval T_{e} of 0.2 ms; and number of echoes N_{ECH} of 12000.

In the NMR experiments, ultra-pure water without impurities was used, and it can be assumed that the physical parameters of the core, such as permeability and porosity, did not undergo significant changes during the process of saturation with ultra-pure water and subsequent drying. After saturating the core with ultra-pure water,

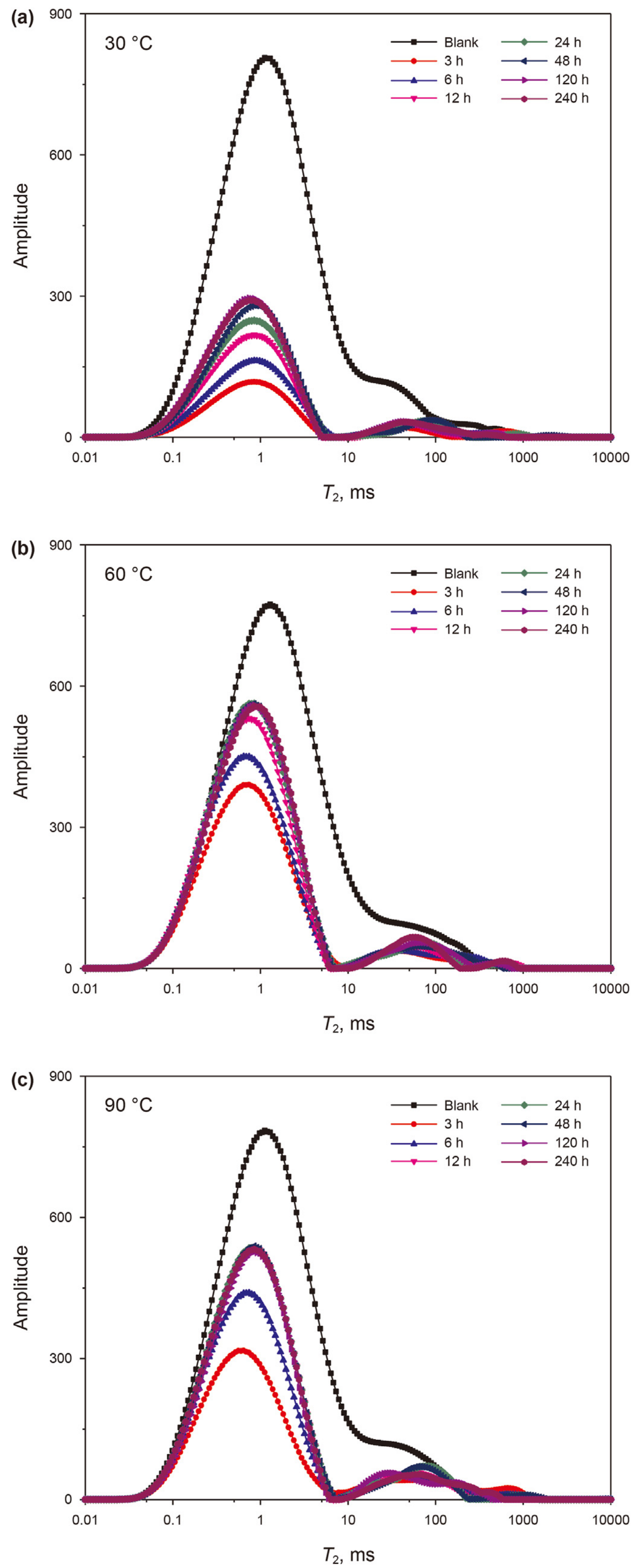

Fig. 9. Impact of temperature on spontaneous imbibition.

NMR equipment was employed to obtain information about the fluid distribution of the core. Subsequently, after drying the core, it was saturated with fluorine oil. By measuring NMR spectra under different experimental conditions and comparing the changes in hydrogen species intensity in the T_2 spectra, the study aimed to investigate the distribution and utilization patterns of fluids within the pore space of the experimental core.

3. Results and discussion

3.1. Interfacial performance

We analyzed the fracturing fluid interfacial properties based on two components: (i) the change of the fluid–liquid interfacial tension between the fracturing fluid and crude oil; (ii) the effect of the fracturing fluid on the rock surface wettability. The fracturing fluid system used in the experiment contained a drainage aid whose main component was the surfactant, which can effectively reduce the oil–water interfacial tension and improve the wettability of the core surface. Fig. 4 presents the corresponding results.

As is shown in Fig. 4, the drainage aid can effectively reduce the oil–water interfacial tension, with significant reductions following an increase in the drainage aid concentration. The interfacial tension reaches a minimum value of 1.23 mN/m at the drainage aid concentration of 0.25 wt%. Following this, the interfacial tension increases gradually with the drainage aid concentration until it finally stabilizes.

The drainage aid can effectively improve the wettability of the core, and the adsorption of the surfactant component in the drainage aid on the core surface achieves this effect. After the lipophilic modifications, the contact angle of the core surface is 122.3°, the core is lipophilic. As the concentration of the drainage aid increases, the final core contact angle decreases to 33.5°, and the surface is both hydrophilic and oleophilic. This corresponds to a drainage aid concentration of 0.25 wt%. The wetting angle then increases gradually with the concentration and finally stabilizes. The change pattern follows that of the interfacial tension.

3.2. Static imbibition results

Static imbibition experiments were conducted using solution A (anti-swell agent and drainage aid), solution B (simulation formation water) and solution C (slickwater fracturing water), respectively. The permeability of the core was approximately 0.3 mD. The imbibition temperature was 60 °C. According to Eq. (1), the static imbibition recovery of the core was calculated under different imbibition solution conditions to obtain the curve of the static imbibition recovery with time (Fig. 5).

As shown in Fig. 5, after 30 min of imbibition, solution A produced the most oil of the core as the imbibition solution, followed by solution C, while solution B produced the least oil. As the imbibition process proceeded, solution A had the strongest imbibition capacity, with a final recovery of 54.37%, followed by solution C, with a final recovery of 38.21%, and solution B maintained the lowest imbibition recovery at 25.72%. By reducing the oil–water interfacial tension and improving the wettability of the core surface, the drainage aid effectively enhances the imbibition ability of the imbibition fluid. The core matrix surface typically exhibits hydrophobic and lipophilic behavior, and saturated oil adsorbs on the core wall surface, making it difficult to be transported. Surfactant adsorption on the core surface improves the wall wettability and reduces the adsorption force between the pore throat wall surface and saturated oil, facilitating the stripping of the crude oil by the imbibition fluid. The surfactants reduce the oil–water interfacial tension between the imbibition fluid and saturated oil. Moreover,

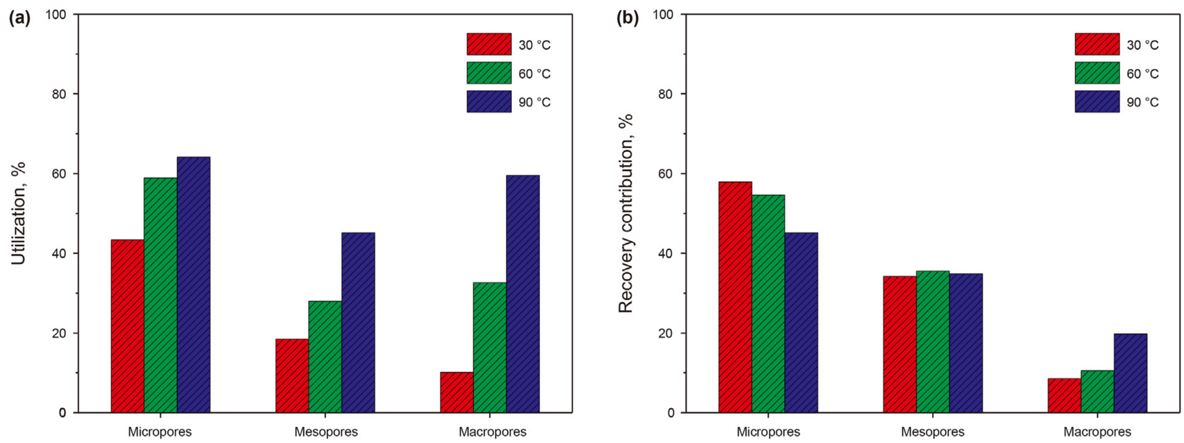

Fig. 10. Fluid utilization and recovery contribution for different pore conditions.

due to the existence of both hydrophilic and hydrophobic groups in its molecular structure, it forms an oil-in-water emulsion, which makes the oil beads from the imbibition fluid easily detach from the core surface. It also effectively improves the transport ability of the saturated oil after the stripping and formation of oil droplets. This greatly increases the imbibition recovery rate.

The anti-swell agent added to solution A effectively weakens the hydration swelling of clay minerals on the surface of the core matrix pore throat. When the saturated crude oil is displaced by imbibition, the contact between the simulated water and clay minerals leads to the occurrence of hydration swelling. In addition, the significantly increased volume of clay minerals reduces the pore throat diameter, while the experimentally used cores are all low-permeability dense cores with a small pore throat diameter and complex pore structure. The increased clay mineral volume further harms the core, thus blocking the matrix pore throat. This makes it difficult for the imbibition fluid to enter the interior of the matrix and for the saturated oil to be transported, leading to a significant reduction in the imbibition fluid sweeping efficiency, which can only act on the surface of the core. The clay anti-swell agent can effectively weaken the hydration swelling and core damage. This allows the imbibition fluid to enter the deep part of the matrix, effectively improving the imbibition fluid sweeping efficiency.

The imbibition recovery of solution C is lower than that of solution A but higher than that of solution B. This can be attributed to the polymeric drag reducing agent added to the slickwater fracturing fluid, which is a solid-phase component insoluble in water. During the imbibition process, small molecule polymers enter the matrix, and the low permeability and small pore throat diameter of the core can block the solid-phase components of its matrix pore throat. This consequently affects its imbibition and oil discharge process, reducing the imbibition recovery rate.

The imbibition recovery rate curve with time was used to calculate the imbibition recovery rate under different imbibition fluid conditions (Fig. 6).

The imbibition recovery rate of different imbibition fluids exhibits a rapid increase to the maximum value at the early stage of imbibition, followed by a marked reduction (Fig. 6). When the imbibition time is greater than 120 h, the imbibition recovery rate is close to 0, indicating that most of the oil recovered by imbibition comes from the early imbibition stage. In particular, at the early stage of imbibition, the imbibition fluid acts on the surface of the core, and the contact area between the matrix and imbibition fluid is maximized, corresponding to the highest imbibition efficiency. Furthermore, the pore throat structure close to the outer surface of the core is relatively simple and exhibits a better connectivity with the outside world. Thus, the saturated oil located inside has the strongest flow capacity. On the other hand, at the early stage of imbibition, the imbibition fluid, as an external phase, is less harmful to the core matrix. Therefore, the recovery rate in the early stage of imbibition rises rapidly to the highest value under multiple effects. As the imbibition proceeds, the imbibition fluid enters the interior of the core, the contact area between the imbibition fluid and the matrix decreases significantly. Thus, the connectivity between the deep pore throat of the matrix and the outside world is reduced. The damage of the imbibition fluid to the matrix consequently intensifies, which in turn leads to a rapid decrease in the imbibition recovery rate.

Moreover, the change pattern of the imbibition recovery rate curve affected by the imbibition solution is consistent with the change pattern of the imbibition recovery. More specifically, solutions B and A have the lowest and highest imbibition recovery rates, respectively, while that of solution C lies between the two. The imbibition recovery rate can also characterize the imbibition performance and imbibition solution drainage, and the imbibition recovery rate increases with the imbibition and drainage performance.

3.3. *Impact of different factors on the oil utilization degree during static imbibition*

Through NMR, T_2 spectra of cores under different static imbibition conditions were obtained. This allowed us to further investigate the variation of different pore size utilization and recovery contribution values with the influencing factors following the core imbibition. The impact of the reducing agent concentration, imbibition temperature, core permeability and fracture development degree on the imbibition of slickwater fracturing fluid was then evaluated.

3.3.1. *Concentration of the drag reducing agent*

Experiments were conducted to investigate the variations in of the T_2 spectrum of the core imbibition process at the drag reducing agent concentration of 0, 0.15, 0.20, and 0.30 wt%, respectively (Fig. 7). This aimed to clarify the variation of the utilization pattern for the static imbibition process of slickwater fracturing fluid under different drag reducing agent concentration conditions.

The experimental results show that the peak value and peak area of the NMR signal intensity in different pore conditions

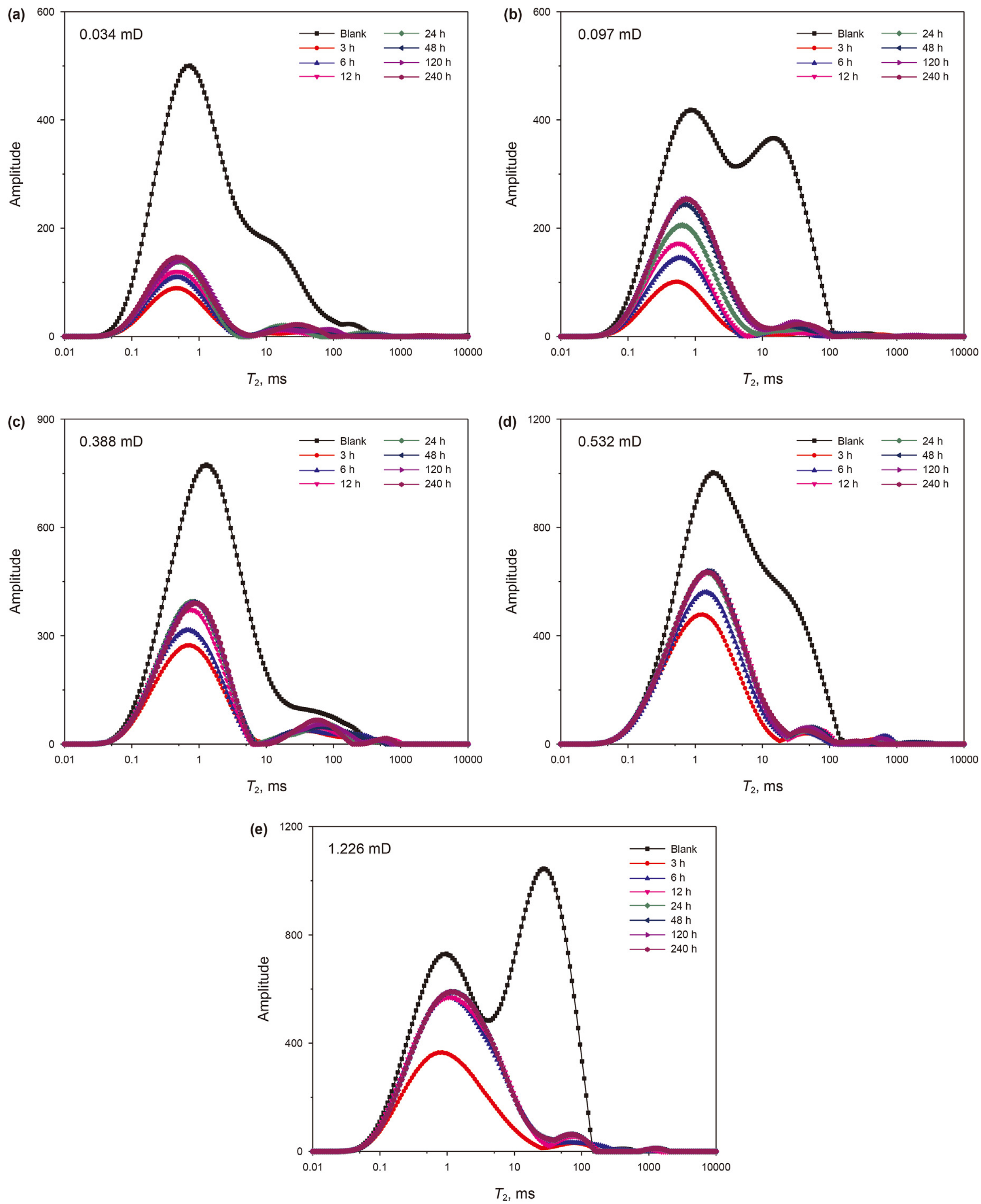

Fig. 11. Impact of core permeability on spontaneous imbibition.

decrease significantly with the increase of the drag reducing agent concentration in the slickwater fracturing fluid. In particular, the most obvious change is in the small pore size range. This indicates that the increase in the concentration of the drag reducing agent has the most prominent effect on small pores.

The degree of utilization and the oil recovery contribution of different pore sizes under different drag reducing agent concentrations during imbibition were further calculated based on T_2 spectra (Fig. 8).

Fig. 8 reveals that the degree of saturated oil utilization under different pore size conditions decreases significantly as the drag reducing agent concentration increases. The drag reducing agent concentration in slickwater fracturing fluid increases from 0 to 0.30 wt%, and the degree of large and medium pore utilization decreases by 8.07% (from 46.83% to 38.76%) and 30.42% (from 55.57% to 25.15%, respectively. Moreover, the large porosity decreases from 81.17% to 33.29% (47.88% decrease), while the medium and small porosity decrease significantly. This indicates that the polymer in the fracturing fluid has a significant effect on the small and medium pores. The significant decrease in the small and

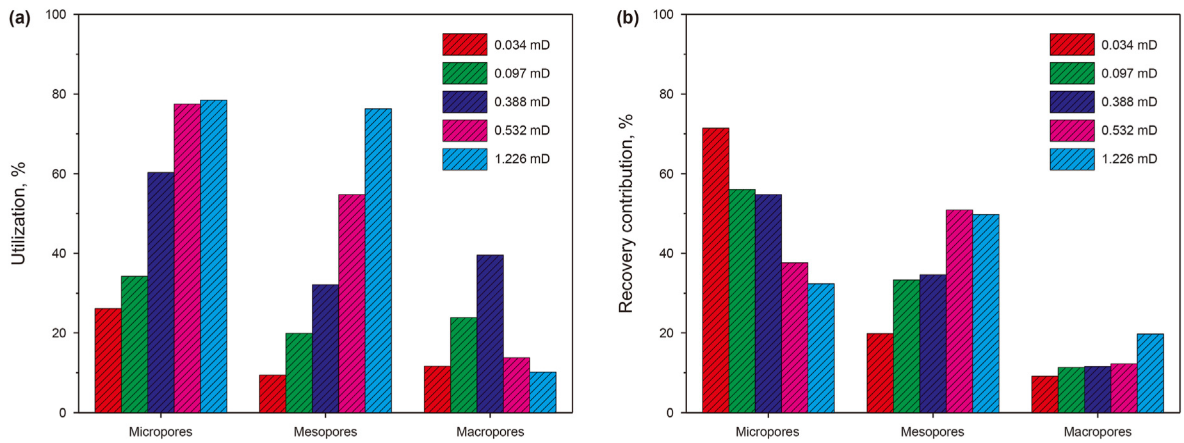

Fig. 12. Fluid utilization and recovery contribution under different pore conditions.

medium pore utilization degree results in a significant increase in the contribution of large pore oil recovery (from 8.05% to 23.7%).

The increase in the concentration of the drag reducing agent enhances its solid-phase component. This in turn blocks the pore space and leads to a significant decrease in the pore throat connectivity, as well as a decrease in the fluid flow properties in the matrix pore space and the degree of saturated oil utilization in different pore sizes. This consequently reduces the imbibition recovery rate. During the imbibition process, the solid-phase component is most likely to block the medium pore space, and the small pore space is also sensitive to the solid-phase component due to its relatively poor connectivity. At the same time, the saturated fluid in the large pore space is more fluid. Therefore, although the solid-phase component in the pore space reduces its connectivity, part of the saturated oil in the large pore space can still be displaced by the imbibition fluid, which leads to a smaller decrease in the utilization degree of the large pore space compared to that of the small and medium pore spaces.

3.3.2. Imbibition temperature

The imbibition temperature also has a significant effect on the imbibition of the slickwater fracturing fluid. NMR experiments were conducted to investigate the changes in T_2 spectra of the core imbibition process under the imbibition temperatures of 30, 60, and 90 °C, respectively (Fig. 9). The changes in the static imbibition pattern of slickwater fracturing fluid under different imbibition temperature conditions were then evaluated.

T_2 spectra of core samples reveal the peak intensity and peak area of the NMR hydrogen signal of the cores to increase with the imbibition temperature. In addition, the stabilization time of the NMR signal curve is reduced at higher temperatures. This indicates that the higher the imbibition temperature, the faster the imbibition rate of the slickwater fracturing fluid.

The degree of the imbibition fluid utilization and recovery contribution with the imbibition temperature were calculated for different pore sizes based on T_2 spectra of core samples (Fig. 10).

As the imbibition temperature increases, the degree of saturated oil utilization for different pore sizes increases significantly, with the change of large pores being the most obvious. When the imbibition temperature increases from 30 to 90 °C, the degree of utilization of small, medium and large pores increases from 43.88% to 65.27% (21.38% increase), 21.33%–48.01% (27.48% increase) and 15.24%–65.32% (50.08% increase), respectively. As the increase in large pore space is significantly larger than those of the medium and small pore spaces, the contribution of the imbibition recovery is also larger. However, due to the small percentage of large pore spaces in tight and low permeability cores, this difference is not obvious.

The increase in temperature significantly reduces the viscosity of the imbibition fluid and oil also enhances their fluidity. This consequently improves the imbibition and displacement performance of the imbibition fluid and increases its sweeping efficiency. The experimental results reveal that the increase in the imbibition temperature effectively improves the imbibition recovery rate. The effect of the imbibition temperature on the recovery rate can be attributed to the improved fluid viscosity and enhanced fluidity, allowing for the easier usage of the saturated oil in the pore space. The most obvious effect is on the large pore space with a better flowability and connectivity. Furthermore, the increase in imbibition temperature further reduces the interfacial tension between the imbibition fluid and the oil, which improves the stripping and transport performance of the crude oil in the large pore space. Due to the small diameter of the pore throat, the medium and small pores generally rely on capillary force to replace the imbibition fluid, and the imbibition temperature (to a certain extent) to improve its fluidity. However, due to the size and connectivity restrictions, the medium and small pores make a smaller contribution to the enhanced imbibition and utilization degree compared to the large pores.

3.3.3. Permeability of the core sample

The physical properties of cores have a significant influence on the performance of the slickwater fracturing fluid imbibition. T_2 spectra of the imbibition process of tight cores with a permeability ranging from 0.05 to 1.0 mD were investigated using NMR to clarify the influence of different core permeabilities on the static imbibition of slickwater fracturing fluid (Fig. 11).

The increase in core permeability results in the significant increase in the core NMR signal under saturated water, and the proportion of the large pore area is enhanced accordingly. This indicates that the core pore volume also increases significantly. Furthermore, as the core permeability increases, the rise in the NMR signal of the small pores is significantly larger than that of the large pores, and the stabilization time of T_2 curves is faster. This can be attributed to the ability of the higher permeability to significantly improve the small pore connectivity, while the saturated oil in the small pores becomes more fluent and easier to use.

The utilization degree of saturated oil and the contribution to the recovery were calculated for different core permeabilities based on T_2 spectra of core samples (Fig. 12).

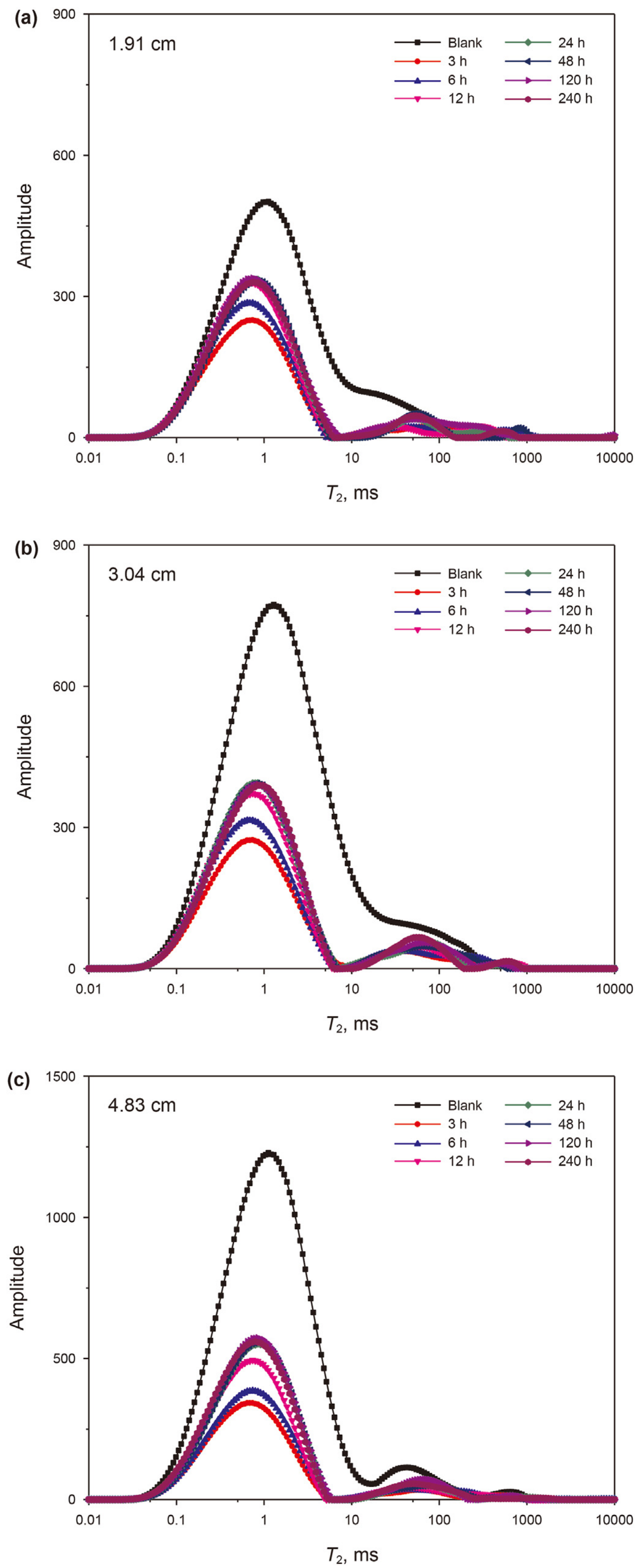

Fig. 13. Impact of the core fracture development on spontaneous imbibition.

The medium and small pore utilization degree increased significantly with the core permeability, while the large pore utilization degree initially increased and subsequently decreased. When the core permeability increased from 0.034 to 1.226 mD, the small pore utilization degree increased from 25.88% to 78.10% (52.22% increase), while the medium pore increased from 9.08% to 75.37% (66.29% increase), and the maximum large pore utilization degree reached 38.38%. As the core permeability increases, there is a higher proportion of large pore NMR signal. This increase in large pore signals indicates enhanced fluid mobilization within the medium and large pore. Consequently, the contribution of fluid utilization from medium and large pores is elevated, while the contribution from small pores decreases.

The higher permeability of the core indicates an improved pore structure and larger pore throat diameter, which significantly increases the fluidity of the saturated oil in the medium and small pores and facilitates the imbibition. Therefore, the degree of saturated oil utilization in the medium and small pores increases significantly. In addition, the pore diameter of relatively high permeability cores expands, which reduces the role of the capillary force in the repulsion process. The larger pore throat diameter also indicates that the solid-phase components in the imbibition fluid can easily enter the matrix, damaging the solid-phase. Thus, the utilization degree of the large pore space initially increases and subsequently decreases with the increasing permeability.

3.3.4. Degree of fracture development

The shorter the core length, the larger the surface area per unit volume of the matrix, indicating more fracture development. Experiments were conducted to investigate the changes in T_2 spectra for the core imbibition process under the core lengths of 1.91, 3.04, and 4.83 cm, respectively (Fig. 13). The changes in the static imbibition pattern of slickwater fracturing fluid with different degree of fracture development were then evaluated.

The core NMR signal intensity under saturated water conditions increases significantly with the core length. However, the change in the NMR signal intensity during imbibition only increases slightly, indicating that the imbibition recovery rate decreases significantly as the core length increases. Further analysis of the imbibition utilization degree and recovery contribution with the core length were performed for different pore sizes (Fig. 14).

As the core length increases, the saturated oil utilization degree of different pore sizes decreases, with the most obvious changes observed for the medium and small pores. The core length increases from 1.91 to 4.83 cm, while the utilization degree of small, medium and large pores decreases from 81.58% to 40.52% (41.06% decrease), 43.85%–29.10% (14.75% decrease), and 40.58%–35.45% (5.13%), respectively. The oil recovery contribution of the small pore space is reduced due to the significant decrease in the utilization degree, while the oil recovery contribution of the large and medium pore spaces increases slightly with the increasing core length.

When the imbibition conditions are determined, the imbibition fluid essentially enters the core matrix at the same depth. The enhanced core length increases the contact area between the matrix and the imbibition fluid, as well as the core volume. The increase in core volume is obviously faster than that of the surface area. More specifically, there is a reduction in the surface area per unit volume of the core and the imbibition fluid sweeping efficiency. This in turn decreases the pore utilization for the different sized pores. Furthermore, the increased core length results in a more complex pore throat structure to a certain extent, while the connectivity of medium and small pores is weakened, and the pores located in the deep part of the matrix cannot be fully utilized. The combination of these factors leads to a significant decrease in the utilization degree with increasing core length.

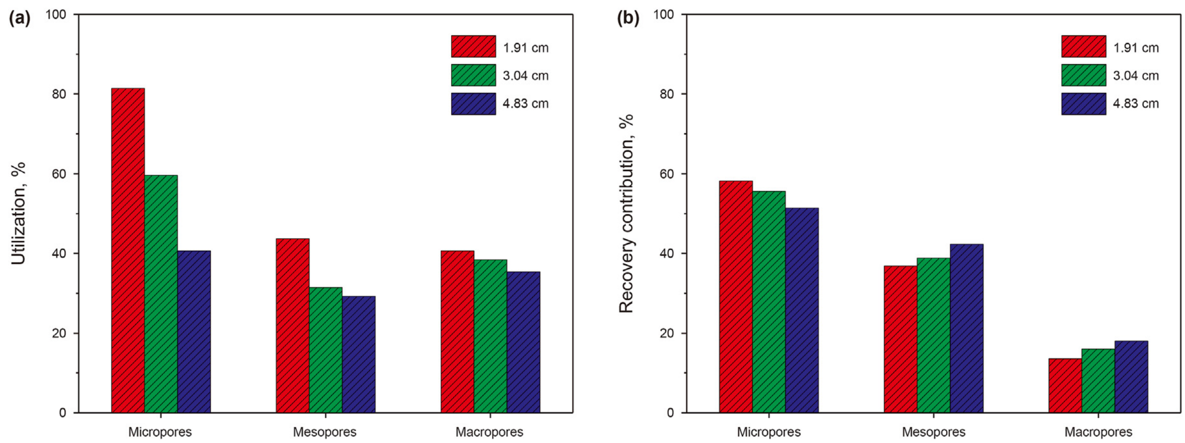

Fig. 14. Fluid utilization and recovery contribution under different pore conditions.

4. Conclusions

This study investigated the degree of core fluid utilization using an online NMR system. The drag reducing agent concentration, formation temperature, core permeability and core fracture development degree were observed to affect the static imbibition. Based on the results, the following key conclusions were determined:

(1) The slickwater fracturing fluid used in the experiment exhibits excellent imbibition and oil displacement capabilities, achieving an imbibition recovery rate of 38.21% after fracturing, compared to a recovery rate of only 25.72% for simulated formation water.
(2) Increasing the concentration of the drag reducing agent results in larger solid-phase components in the imbibition solution. These solid-phase components are more prone to block small and medium-sized pores, thereby reducing the fluid mobilization in these pores.
(3) Elevated temperature improves fluid mobility. Notably, the fluid mobility in larger pores increases significantly compared to that in smaller pores, leading to an enhanced fluid mobilization.
(4) An increase in permeability indicates improved pore conductivity. As a result, fluid mobilization in various pores increases. Excessive permeability results in a significant influx of solid-phase components into macropores, causing damage to the solid phase and consequently reducing the fluid mobilization in larger pores.
(5) With an increase in the core length, the surface area per unit volume of the core decreases. This indicates reduced fracture development. In addition, the internal structure of the core becomes more complex, impeding fluid mobilization within the core. Consequently, the degree of pore mobilization decreases for all pore sizes.

Declaration of competing interest

The authors declare that they have no known competing financial interests or personal relationships that could have appeared to influence the work reported in this paper.

Acknowledgment

The authors sincerely appreciate the financial support from the National Natural Science Foundation of China (No. 52074279, 51874261).

References

Abaa, K., Wang, J., Elsworth, D., Ityokumbul, M., 2022. Laboratory investigation of impact of slickwater composition on multiphase permeability evolution in tight sandstones. SPE Prod. Oper. 37 (2), 202–217. https://doi.org/10.2118/180250-PA.
Al-Muntasheri, G.A., 2014. A critical review of hydraulic-fracturing fluids for moderate- to ultralow-permeability formations over the last decade. SPE Prod. Oper. 29 (4), 243–260. https://doi.org/10.2118/169552-PA.
Al-Muntasheri, G.A., Li, L.M., Liang, F., Gomaa, A.M., 2018. Concepts in cleanup of fracturing fluids used in conventional reservoirs: a literature review. SPE Prod. Oper. 33 (2), 196–213. https://doi.org/10.2118/186112-PA.
Barati, R., Liang, J.-T., 2014. A review of fracturing fluid systems used for hydraulic fracturing of oil and gas wells. J. Appl. Polym. Sci. 131 (16). https://doi.org/10.1002/app.40735.
Cai, J.C., Li, C.X., Song, K.P., et al., 2020. The influence of salinity and mineral components on spontaneous imbibition in tight sandstone. Fuel 269, 117087. https://doi.org/10.1016/j.fuel.2020.117087.
Cheng, Z.L., Ning, Z.F., Yu, X.F., Wang, Q., Zhang, W.T., 2019. New insights into spontaneous imbibition in tight oil sandstones with NMR. J. Petrol. Sci. Eng. 179, 455–464. https://doi.org/10.1016/j.petrol.2019.04.084.
Dai, C.L., Cheng, R., Sun, X., et al., 2019. Oil migration in nanometer to micrometer sized pores of tight oil sandstone during dynamic surfactant imbibition with online NMR. Fuel 245, 544–553. https://doi.org/10.1016/j.fuel.2019.01.021.
Fall, A., Eichhubl, P., Bodnar, R.J., Laubach, S.E., Davis, J.S., 2015. Natural hydraulic fracturing of tight-gas sandstone reservoirs, Piceance Basin, Colorado. GSA Bulletin 127 (1–2), 61–75. https://doi.org/10.1130/B31021.1.
Guo, C.H., Xu, J.C., Wei, M.Z., Jiang, R.Z., 2015. Experimental study and numerical simulation of hydraulic fracturing tight sandstone reservoirs. Fuel 159, 334–344. https://doi.org/10.1016/j.fuel.2015.06.057.
Guo, J.C., Li, M., Chen, C., Tao, L., Liu, Z., Zhou, D.S., 2020. Experimental investigation of spontaneous imbibition in tight sandstone reservoirs. J. Petrol. Sci. Eng. 193, 107395. https://doi.org/10.1016/j.petrol.2020.107395.
Haynes, A.K., Clough, M.D., Fletcher, A.J., Weston, S., 2013. The successful implementation of a novel polymer EOR pilot in the low permeability Windalia Field. In: SPE Enhanced Oil Recovery Conference. https://doi.org/10.2118/165253-MS.
Hossain, M.M., Rahman, M.K., 2008. Numerical simulation of complex fracture growth during tight reservoir stimulation by hydraulic fracturing. J. Petrol. Sci. Eng. 60 (2), 86–104. https://doi.org/10.1016/j.petrol.2007.05.007.
Jiang, Z.H., Liu, Z.D., Zhao, P.Q., et al., 2022. Evaluation of tight waterflooding reservoirs with complex wettability by NMR data: a case study from Chang 6 and 8 members, Ordos Basin, NW China. J. Petrol. Sci. Eng. 213, 110436. https://doi.org/10.1016/j.petrol.2022.110436.
Jiang, Z.H., Li, G.R., Zhao, P.Q., et al., 2023. Study on spontaneous imbibition and displacement characteristics of mixed-wet tight sandstone reservoir based on high-precision balance and NMR method. Fuel 345, 128247. https://doi.org/10.1016/j.fuel.2023.128247.
King, G.E., 2012. Hydraulic fracturing 101: what every representative, environmentalist, regulator, reporter, investor, university researcher, neighbor and engineer should know about estimating frac risk and improving frac performance in unconventional gas and oil wells. In: SPE Hydraulic Fracturing Technology Conference. https://doi.org/10.2118/152596-MS.
Lei, Q., Weng, D.W., Luo, J.H., et al., 2019. Achievements and future work of oil and gas production engineering of CNPC. Petrol. Explor. Dev. 46 (1), 145–152. https://doi.org/10.1016/S1876-3804(19)30014-X.
Leon, J.M., Castillo, A.F., Perez, R., et al., 2018. A successful polymer flood pilot at

Palogrande-Cebu, a low permeability reservoir in the Upper Magdalena Valley, Colombia. In: SPE Improved Oil Recovery Conference. https://doi.org/10.2118/190165-MS.
Li, Z.S., Yao, Y.B., Zhang, C., Liu, Y., 2023. A novel method for evaluation of the spontaneous imbibition process in tight reservoir rocks: mathematical model and experimental verification. Geoenergy Sci. Eng. 223, 211554. https://doi.org/10.1016/j.geoen.2023.211554.
Liu, C., Li, Y.Y., Wang, P., et al., 2022. Preparation and performance evaluation of nano-composite fracturing fluid with good oil displacement ability in tight reservoir. J. Mol. Liq. 367, 120494. https://doi.org/10.1016/j.molliq.2022.120494.
Liu, C., You, Q., Wang, T.R., et al., 2024. Study of microscopic imbibition and formation plugging mechanism of the compact oil reservoir based on SEM and NMR analysis. Fuel 357, 129672. https://doi.org/10.1016/j.fuel.2023.129672.
Liu, M., Xie, R.H., Li, J., et al., 2023. A new NMR-data-based method for predicting petrophysical properties of tight sandstone reservoirs. Energy Geosci. 4 (2), 100083. https://doi.org/10.1016/j.engeos.2021.12.002.
Liu, S., Ni, J., Wen, X.L., et al., 2020. A dual-porous and dual-permeable media model for imbibition in tight sandstone reservoirs. J. Petrol. Sci. Eng. 194, 107477. https://doi.org/10.1016/j.petrol.2020.107477.
Montgomery, C.T., Smith, M.B., 2010. Hydraulic fracturing: history of an enduring technology. J. Petrol. Technol. 62 (12), 26–40. https://doi.org/10.2118/1210-0026-JPT.
Rachapudi, R.V., , et al.Alshehhi, S.S., BinAmro, A.A., et al., 2020. World first polymer injectivity test in high salinity and high temperature carbonate reservoir, case study from a giant reservoir in UAE. In: Abu Dhabi International Petroleum Exhibition & Conference. https://doi.org/10.2118/203405-MS.
Song, H.F., Ghosh, P., Mohanty, K., 2021. Transport of polymers in low permeability carbonate rocks. In: SPE Annual Technical Conference and Exhibition. https://doi.org/10.2118/206024-MS.
Tang, W.-Y., Sheng, J.J., Jiang, T.-X., 2023. Further discussion of CO_2 huff-n-puff mechanisms in tight oil reservoirs based on NMR monitored fluids spatial distributions. Petrol. Sci. 20 (1), 350–361. https://doi.org/10.1016/j.petsci.2022.08.014.
Vishkai, M., Gates, I., 2019. On multistage hydraulic fracturing in tight gas reservoirs: montney Formation, Alberta, Canada. J. Petrol. Sci. Eng. 174, 1127–1141. https://doi.org/10.1016/j.petrol.2018.12.020.
Wang, C., Gao, H., Gao, Y., Fan, H.M., 2020. Influence of pressure on spontaneous imbibition in tight sandstone reservoirs. Energy Fuel. 34 (8), 9275–9282. https://doi.org/10.1021/acs.energyfuels.0c00639.
Wu, B.H., Xie, R.H., Wang, X.Y., Wang, T.Y., Yue, W.Z., 2020. Characterization of pore structure of tight sandstone reservoirs based on fractal analysis of NMR echo data. J. Nat. Gas Sci. Eng. 81, 103483. https://doi.org/10.1016/j.jngse.2020.103483.
Wu, Z.W., Cui, C.Z., Jia, P.F., Wang, Z., Sui, Y.F., 2022. Advances and challenges in hydraulic fracturing of tight reservoirs: a critical review. Energy Geosci. 3 (4), 427–435. https://doi.org/10.1016/j.engeos.2021.08.002.
Xia, Y.X., Tian, Z.H., Xu, S., Wei, W., Cai, J.C., 2021. Effects of microstructural and petrophysical properties on spontaneous imbibition in tight sandstone reservoirs. J. Nat. Gas Sci. Eng. 96, 104225. https://doi.org/10.1016/j.jngse.2021.104225.
Xu, D.R., Bai, B.J., Wu, H.R., et al., 2019. Mechanisms of imbibition enhanced oil recovery in low permeability reservoirs: effect of IFT reduction and wettability alteration. Fuel 244, 110–119. https://doi.org/10.1016/j.fuel.2019.01.118.
Yang, Z.M., Liu, X.W., Li, H.B., et al., 2019. Analysis on the influencing factors of imbibition and the effect evaluation of imbibition in tight reservoirs. Petrol. Explor. Dev. 46 (4), 779–785. https://doi.org/10.1016/S1876-3804(19)60235-1.
Yang, K., Wang, F.-Y., Zhao, J.-Y., 2023. Experimental study of surfactant-enhanced spontaneous imbibition in fractured tight sandstone reservoirs: the effect of fracture distribution. Petrol. Sci. 20 (1), 370–381. https://doi.org/10.1016/j.petsci.2022.09.033.
Zheng, X.Q., Shi, J.F., Cao, G., et al., 2022. Progress and prospects of oil and gas production engineering technology in China. Petrol. Explor. Dev. 49 (3), 644–659. https://doi.org/10.1016/S1876-3804(22)60054-5.
Zhou, B., You, Q., Li, Y.Y., et al., 2022. Preparation and performance evaluation of an active nanofluid for enhanced oil recovery in ultra-low permeability reservoirs. J. Mol. Liq. 347, 118331. https://doi.org/10.1016/j.molliq.2021.118331.
Zou, C., 2013. Unconventional Petroleum Geology. Unconventional Petroleum Geology. Elsevier Inc.
Zou, C.N., Yang, Z., Tao, S.Z., et al., 2012. Nano-hydrocarbon and the accumulation in coexisting source and reservoir. Petrol. Explor. Dev. 39 (1), 15–32. https://doi.org/10.1016/S1876-3804(12)60011-1.
Zou, C.N., Zhang, G.S., Yang, Z., et al., 2013. Geological concepts, characteristics, resource potential and key techniques of unconventional hydrocarbon: on unconventional petroleum geology. Petrol. Explor. Dev. 40 (4), 385–399+454. https://doi.org/10.11698/PED.2013.04.01.